



Supporting Information

for *Adv. Sci.*, DOI: 10.1002/advs.202001596

The beneficial role of Sunitinib in tumor immune surveillance by regulating tumor PD-L1

*Hui Li, Xinwei Kuang, Long Liang, Youqiong Ye, YongChang Zhang, Jialu Li,
Fangyu Ma, Juan Tao, Guang Lei, Shuang Zhao, Juan Su, Nong Yang, Cong Peng,
Xiaowei Xu, Mien-Chie Hung, Leng Han*, Hong Liu*, Jing Liu*, Xiang Chen**

The beneficial role of Sunitinib in tumor immune surveillance
by regulating tumor PD-L1

Hui Li⁺, Xinwei Kuang⁺, Long Liang⁺, Youqiong Ye⁺, YongChang Zhang, Jialu Li, Fangyu Ma, Juan Tao, Guang Lei, Shuang Zhao, Juan Su, Nong Yang, Cong Peng, Xiaowei Xu, Mien-Chie Hung, Leng Han, Hong Liu*, Jing Liu*, Xiang Chen**

Supplemental Table 1. Tumor growth analysis results for Figure 1C, Figure 4D and Supplemental Figure 4C. There are two tables for the data in each figure. The first table summarizes the pairwise comparison p-value at each time point, with a smaller p-value indicating a larger difference between the two groups. The second table presents the results of mixed-effect model fitting as described in Methods. The tumor volume data was log2 transformed before model fitting. For the fixed effect of treatment options, either the control or the combined therapy of interest (eg: Sunitinib +CTLA-4 mAb for Fig 4D) was set as the reference group. The significant interaction effect between time and treatment indicates that the treatment has a higher anti-tumor efficacy as time goes when compared to the control group.

| Pairwise Comparisons at each time point (Fig 1C) | 0 | 3 | 6 | 9 | 12 |
|-------------------------------------------------------------|-----------------|----------|----------------|----------|-----------|
| Su 20 vs. Control | 1 | 0.6548 | 0.2268 | 0.0071 | <0.001 |
| Sun 40 vs. Control | 1 | 0.5324 | 0.0296 | 0.0004 | <0.001 |
| Su 20 vs. Sun 40 | 1 | 0.9768 | 0.4696 | 0.2678 | <0.001 |
| Treatment effect analysis Fig 1C | Estimate | | P value | | |
| Days | 0.42613 | | <0.0001 | | |
| Sun 20 | -0.11767 | | 0.62045 | | |

| | | |
|---------------------|----------|----------|
| Sun 40 | -0.04996 | 0.83400 |
| Weight | -0.04009 | 0.43161 |
| Days: Sun 20 | -0.05058 | <0.00942 |
| Days: Sun 40 | -0.13653 | <0.001 |

| Days Comparisons (Fig 4D) | 0 | 3 | 6 | 9 | 12 |
|---------------------------------------------|----------|----------|----------|----------|-----------|
| Sunitinib+IgG2b vs. Sunitinib+CTLA-4 mAb | 0.9954 | 0.2390 | 0.0112 | <0.0001 | <0.0001 |
| Vehicle+CTLA-4 mAb vs. Sunitinib+CTLA-4 mAb | 0.9992 | 0.2138 | 0.0247 | 0.0002 | <0.0001 |
| Vehicle+IgG2b vs. Sunitinib+CTLA-4 mAb | 0.9972 | <0.0001 | <0.0001 | <0.0001 | <0.0001 |
| Vehicle+CTLA-4 mAb vs. Sunitinib+IgG2b | 0.9831 | 0.9999 | 0.9787 | 0.0442 | <0.0001 |
| Vehicle+IgG2b vs. Sunitinib+IgG2b | 0.9729 | 0.0003 | 0.0225 | 0.0155 | <0.0001 |
| Vehicle+IgG2b vs. Vehicle+CTLA-4 mAb | 0.9999 | 0.0004 | 0.0102 | <0.0001 | <0.0001 |

| Fig 4D | Estimate | P value |
|---------------------------------|-----------------|----------------|
| Days | 0.20728 | <0.0001 |
| Sunitinib+IgG2b | 0.05255 | 0.78854 |
| Vehicle+CTLA-4 mAb | 0.28002 | 0.15591 |
| Vehicle+IgG2b | 0.61890 | 0.00226 |
| Weight | -0.01268 | 0.63811 |
| Days: Sunitinib+IgG2b | 0.23544 | <0.0001 |
| Days: Vehicle+CTLA-4 mAb | 0.15706 | <0.0001 |
| Days: Vehicle+IgG2b | 0.23833 | <0.0001 |

| Days Comparisons (Sup Fig 4C) | 0 | 3 | 6 | 9 | 12 |
|---------------------------------------------|----------|----------|----------|----------|-----------|
| Sunitinib+IgG2b vs. Sunitinib+CTLA-4 mAb | 1.0000 | 0.4000 | 0.0248 | <0.0001 | 0.0001 |
| Vehicle+CTLA-4 mAb vs. Sunitinib+CTLA-4 mAb | 0.9999 | 0.6185 | 0.1880 | 0.0016 | 0.0011 |
| Vehicle+IgG2b vs. Sunitinib+CTLA-4 mAb | 0.9976 | 0.0716 | 0.0001 | <0.0001 | <0.0001 |
| Vehicle+CTLA-4 mAb vs. Sunitinib+IgG2b | 0.9996 | 0.9802 | 0.6960 | 0.3005 | 0.4769 |
| Vehicle+IgG2b vs. Sunitinib+IgG2b | 0.9988 | 0.7180 | 0.0391 | 0.0002 | 0.0005 |
| Vehicle+IgG2b vs. Vehicle+CTLA-4 mAb | 0.9946 | 0.4926 | 0.0043 | <0.0001 | <0.0001 |

| Supplemental Fig 4C | Estimate | P value |
|----------------------------|-----------------|----------------|
| Days | 0.09566 | <0.0001 |
| Sunitinib+IgG2b | -0.02342 | 0.9032 |
| Vehicle+CTLA-4 mAb | -0.05995 | 0.7578 |
| Vehicle+IgG2b | 0.10332 | 0.5936 |
| Weight | 0.08644 | 0.0634 |
| Days: Sunitinib+IgG2b | 0.19625 | <0.0001 |
| Days: Vehicle+CTLA-4 mAb | 0.17227 | <0.0001 |
| Days: Vehicle+IgG2b | 0.24570 | <0.0001 |

Supplemental Table 2. List of significantly differentially-expressed genes that belong to the biological process of selective autophagy.

| Symbol | logFC | logCPM | FDR |
|----------------------|-------------------|-------------------|-----------------|
| <i>SESN2</i> | 1.33843018 | 6.52706829 | 1.07E-44 |
| <i>OPTN</i> | 1.09085167 | 3.57344674 | 1.31E-09 |
| <i>SPTLC1</i> | 0.70923036 | 4.94083565 | 3.38E-08 |
| <i>BECN1</i> | 0.59320344 | 5.33663922 | 1.26E-07 |
| <i>CALCOCO2</i> | 0.69310023 | 4.48507248 | 6.76E-07 |
| <i>MFN2</i> | -0.3981555 | 8.36942453 | 8.76E-07 |
| <i>RNF41</i> | 0.38443553 | 7.29518992 | 3.95E-06 |
| <i>SQSTM1</i> | 0.33166395 | 10.6534671 | 7.24E-05 |
| <i>ADRB2</i> | -0.8594578 | 2.88621709 | 0.00013687 |
| <i>HDAC6</i> | 0.42672627 | 5.41339149 | 0.00018645 |
| <i>HTT</i> | -0.308237 | 7.0191931 | 0.00043588 |
| <i>MAPK3</i> | -0.3207781 | 7.05625063 | 0.00072537 |
| <i>WIPI2</i> | -0.2846679 | 7.44758998 | 0.00106038 |
| <i>HTRA2</i> | -0.2760406 | 6.7645145 | 0.00221018 |
| <i>LGALS8</i> | 0.48193938 | 4.16776755 | 0.00231538 |
| <i>ATG14</i> | 0.59298676 | 3.49286434 | 0.00294681 |
| <i>TOMM7</i> | 0.4029165 | 5.55853603 | 0.00870344 |
| <i>WDFY3</i> | 0.69091522 | 2.38409663 | 0.01245925 |
| <i>RETREG1</i> | 1.27981231 | 0.38610981 | 0.01706579 |
| <i>SMURF1</i> | -0.2553462 | 5.78289634 | 0.01842524 |
| <i>UBQLN1</i> | 0.22730394 | 6.32636441 | 0.02312429 |
| <i>VPS13C</i> | 0.7992966 | 1.23922786 | 0.0409454 |
| <i>NOD1</i> | -0.3949972 | 3.68872132 | 0.04170285 |
| <i>ATG16L1</i> | -0.2580434 | 5.00188992 | 0.04598677 |
| <i>AMBRA1</i> | -0.2022006 | 6.21618481 | 0.04808278 |

SQSTM1 is the p62 as described in the manuscript. logCPM represents the gene's relative expression level averaged across samples. Abbreviations: logFC, log fold change; logCPM, log counts per million; FDR, adjusted p-value after controlling for false discovery rate.

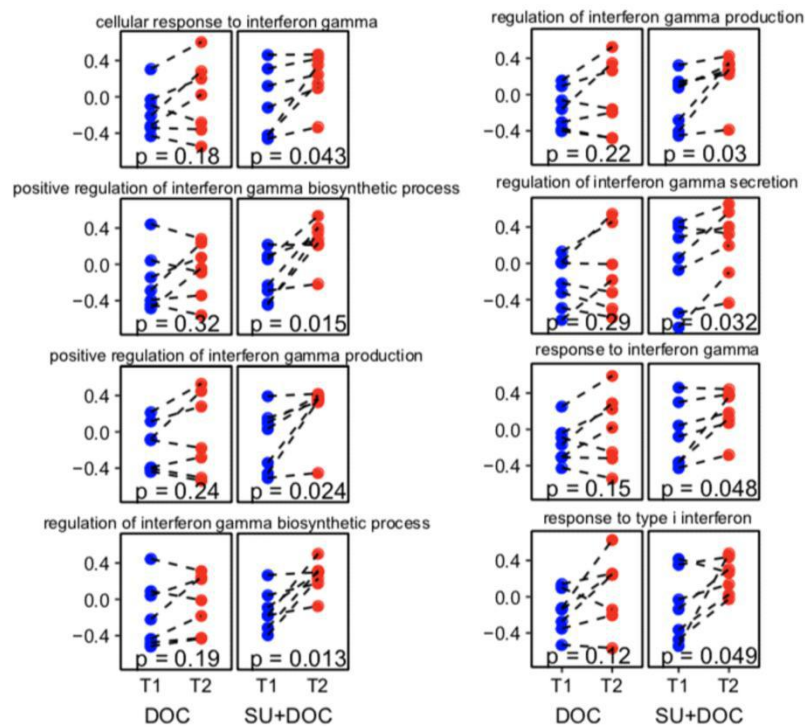
Supplemental Table 3. Clinicopathologic characteristics of anti-PD-1 monotherapy cohorts.

| Patient No. | Response | Gender | Age | Tumor types | TNM stage | PS score | PFS (month) | OS (month) | Adverse effect | Metastatic lesion |
|-------------|----------|--------|-----|-------------|-----------|----------|-------------|------------|--------------------|------------------------------------------|
| 1 | PR | Male | 68 | LUAD | T2N3M1B | 1 | 19 | 53+ | None | Mediastinum, axilla |
| 2 | SD | Male | 50 | LUAD | T2N3M1B | 1 | 10 | 38+ | None | Pleura |
| 3 | SD | Male | 50 | LUAD | T3N3M1 | 1 | 6+ | 17+ | None | Bone liver adrenal gland |
| 4 | SD | Male | 40 | LUAD | T4N3M1 | 1 | 6+ | 41+ | erythra | pleura, multiple bones |
| 5 | PR | Male | 61 | LUSC | T1N3M1B | 1 | 6+ | 15+ | I° hepatic damage | Bone |
| 6 | PR | Male | 57 | LUSC | T2N0M1 | 1 | 4.5+ | 23+ | I° hypothyroidism | Bone |
| 7 | SD | Male | 59 | LUSC | T2N2M1 | 1 | 12 | 15 | I° hepatic damage | Bone |
| 8 | SD | Male | 66 | LUSC | T4N2M1 | 1 | 4.5 | 11+ | None | brain, adrenal gland |
| 9 | PR | Male | 50 | LUSC | T2N3M0 | 1 | 10 | 29+ | epilepsy | Iliac crest, retroperitoneal lymph nodes |
| 10 | SD | Male | 74 | LUSC | T2N2M1 | 1 | 5 | 19 | None | lung, liver |
| 11 | SD | Male | 47 | LUSC | T4N2M03B | 1 | 5 | 15 | None | lung, mediastinal lymph nodes |
| 12 | PD | Male | 57 | LUAD | T2N2M1B | 1 | 1.5 | 11 | I° weak, cough | Bone |
| 13 | PD | Male | 38 | LUAD | T1N3M1B | 1 | 2 | 9 | I° emesis | Bone, adrenal, brain |
| 14 | SD | Male | 63 | LUAD | T1N0M1 | 1 | 3 | 10 | None | lung, abdominal subcutaneous |
| 15 | PD | Female | 54 | LUAD | T3N0M1B | 1 | 2 | 6 | None | lung, bone |
| 16 | PD | Male | 72 | LUSC | T1N3M1 | 1 | 2 | 27+ | arrhythmia | axilla, gluteus maximus, humerus |
| 17 | PD | Male | 62 | LUSC | T1N2M1 | 1 | 1 | 1 | None | Bone |
| 18 | PD | Male | 62 | LUSC | T3N3M0 | 1 | 0.5 | 10 | None | None |
| 19 | PD | Male | 47 | LUSC | T3N2M1a | 1 | 1.5 | 15 | II° hepatic damage | Pleura |

Anti-PD-1, anti-programmed death-1; CR, complete response; PR, partial response; SD, stable disease; PD, progressive disease; PFS, progression-free survival; OS, overall survival. Patients were stratified into response groups based on RECIST 1.1 criteria. Patients with CR, PR, and SD > 3 months were classified as responders, while patients with SD ≤ 3 months and PD were classified as non-responders. LUSC: Lung squamous cell carcinoma. LUAD: Lung adenocarcinoma. TNM stage based on The 8th Edition Lung Cancer Stage Classification.

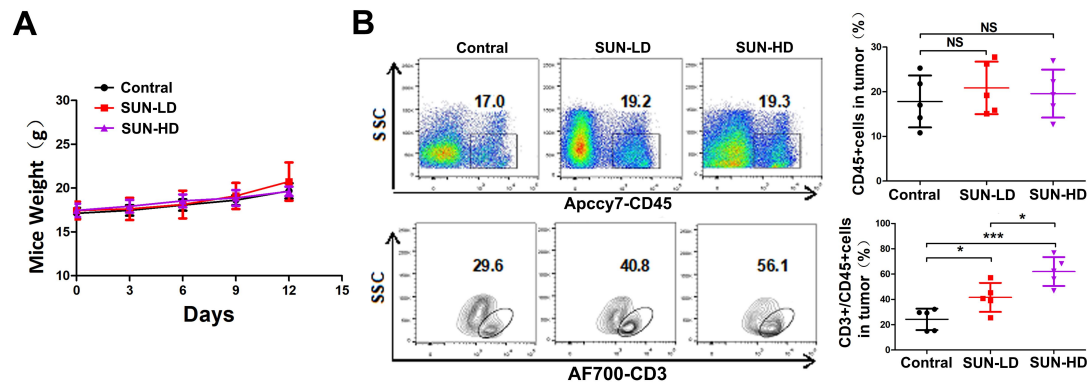
Supplemental Figures

Supplemental Figure 1



Supplemental Figure 1. Docetaxel- and sunitinib + docetaxel-induced changes from baseline in the GSVA of $\text{INF}\gamma$ related GO terms to 14 days after treatment in cancer patients.

Supplemental Figure 2

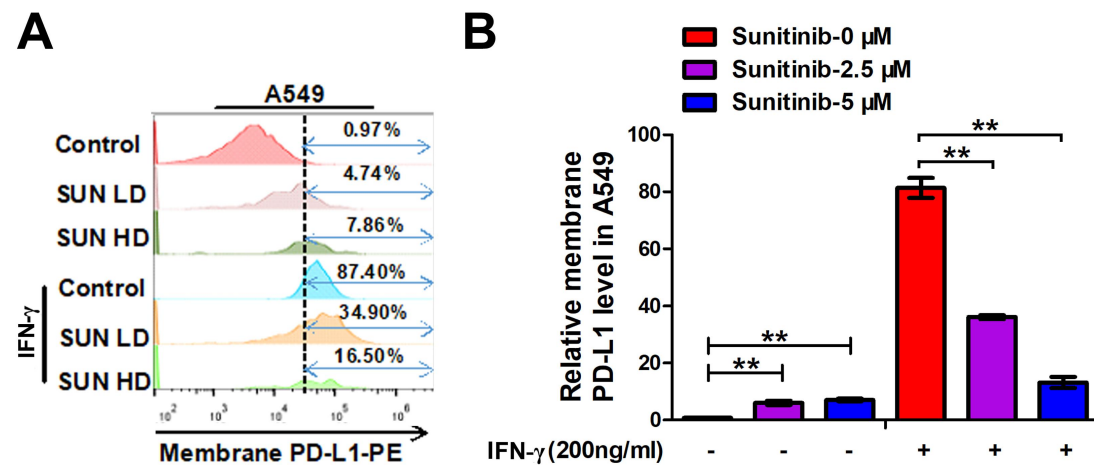


Supplemental Figure 2. Sunitinib increase the CTL population and no effect on mice body weight.

A. During the treatment period, mouse body weight was measured on the indicated time points Data are shown as mean \pm SD.

B. Representative profiles and the quantification of flow cytometry-based detection of CD45+CD3+ CTL in the tumor mass form Sunitinib treatment or vehicle. n=5 mice per group, data represent mean \pm SD, *p<0.05,***p<0.001.

Supplemental Figure 3



Supplemental Figure 3. Sunitinib exposure decreased membrane-located PD-L1 level in melanoma cells and A549 cells.

- A. Representative profiles of flow cytometry analysis of membrane PD-L1 expression by flow-cytometric analysis after increasing concentrations of Sunitinib (2.5 to 5 μ M) treated A549 cells for 24 hours under IFN- γ exposure.
- B. The quantitative analysis of flow cytometry analysis of membrane PD-L1 expression by flow-cytometric analysis after increasing concentrations of Sunitinib (2.5 to 5 μ M) treated A549 cells for 24 hours under IFN- γ exposure.

Supplemental Figure 4

A

| | Term | Ont | N | Up | Down | P.Up | P.Down |
|------------|----------------------------------------|-----|------|-----|------|--------------|-----------|
| G0:0044248 | cellular catabolic process | BP | 1761 | 488 | 390 | 4.784137e-08 | 0.9996886 |
| G0:0009056 | catabolic process | BP | 1940 | 518 | 443 | 3.493355e-06 | 0.9961663 |
| G0:0006914 | autophagy | BP | 410 | 130 | 90 | 1.633475e-05 | 0.9528864 |
| G0:0061919 | process utilizing autophagic mechanism | BP | 410 | 130 | 90 | 1.633475e-05 | 0.9528864 |
| G0:0050662 | coenzyme binding | MF | 220 | 76 | 46 | 1.686749e-05 | 0.9194302 |
| G0:0016236 | macroautophagy | BP | 259 | 88 | 52 | 2.153604e-05 | 0.9803426 |

B

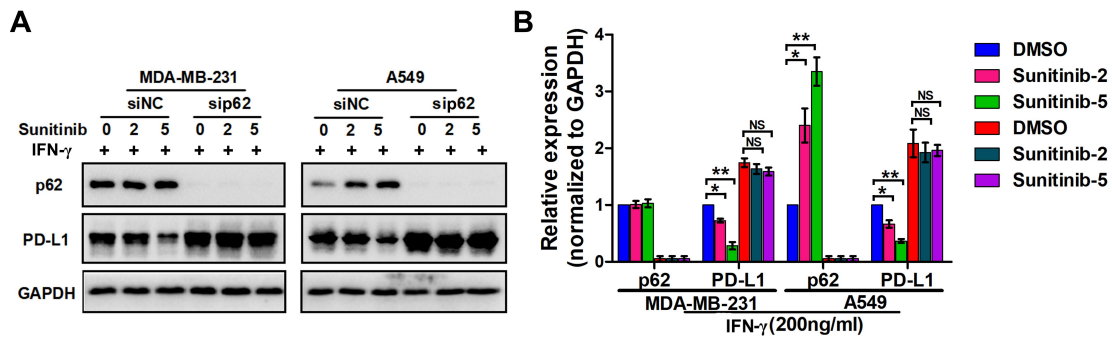
| | Term | Ont | N | Up | Down | P.Up | P.Down | significance |
|------------|-----------------------------------------|-----|-----|-----|------|--------------|-----------|--------------|
| G0:0006914 | autophagy | BP | 410 | 130 | 90 | 1.633475e-05 | 0.9528864 | TRUE |
| G0:0061919 | process utilizing autophagic mechanism | BP | 410 | 130 | 90 | 1.633475e-05 | 0.9528864 | TRUE |
| G0:0016236 | macroautophagy | BP | 259 | 88 | 52 | 2.153604e-05 | 0.9803426 | TRUE |
| G0:0010506 | regulation of autophagy | BP | 264 | 79 | 59 | 4.018038e-03 | 0.8811540 | TRUE |
| G0:0044754 | autolysosome | CC | 8 | 6 | 1 | 5.432286e-03 | 0.9353320 | TRUE |
| G0:0005776 | autophagosome | CC | 79 | 28 | 11 | 7.537421e-03 | 0.9956572 | TRUE |
| G0:0000045 | autophagosome assembly | BP | 84 | 28 | 15 | 9.572792e-03 | 0.9355934 | TRUE |
| G0:1905037 | autophagosome organization | BP | 87 | 29 | 15 | 9.741947e-03 | 0.9588765 | TRUE |
| G0:0016240 | autophagosome membrane docking | BP | 4 | 3 | 0 | 2.439379e-02 | 1.0000000 | TRUE |
| G0:0016241 | regulation of macroautophagy | BP | 145 | 44 | 32 | 2.544329e-02 | 0.8576885 | TRUE |
| G0:0030242 | autophagy of peroxisome | BP | 5 | 3 | 0 | 2.778880e-02 | 1.0000000 | TRUE |
| G0:0032258 | protein localization by the Cvt pathway | BP | 2 | 2 | 0 | 3.698963e-02 | 1.0000000 | TRUE |
| G0:0097352 | autophagosome maturation | BP | 35 | 13 | 6 | 4.425284e-02 | 0.9176229 | TRUE |
| G0:0061912 | selective autophagy | BP | 43 | 15 | 10 | 4.891990e-02 | 0.6791124 | TRUE |

Supplemental Figure 4. Sunitinib induce autophagy in melanoma cells.

A. Top up-regulated GO terms identified from gene ontology analysis using the RNA sequencing data. Note that autophagy is a sub-GO term of catabolic process and cellular catabolic process.

B. List of significantly enriched autophagy-related biological processes or cellular components from the RNA sequencing data analysis.

Supplemental Figure 5

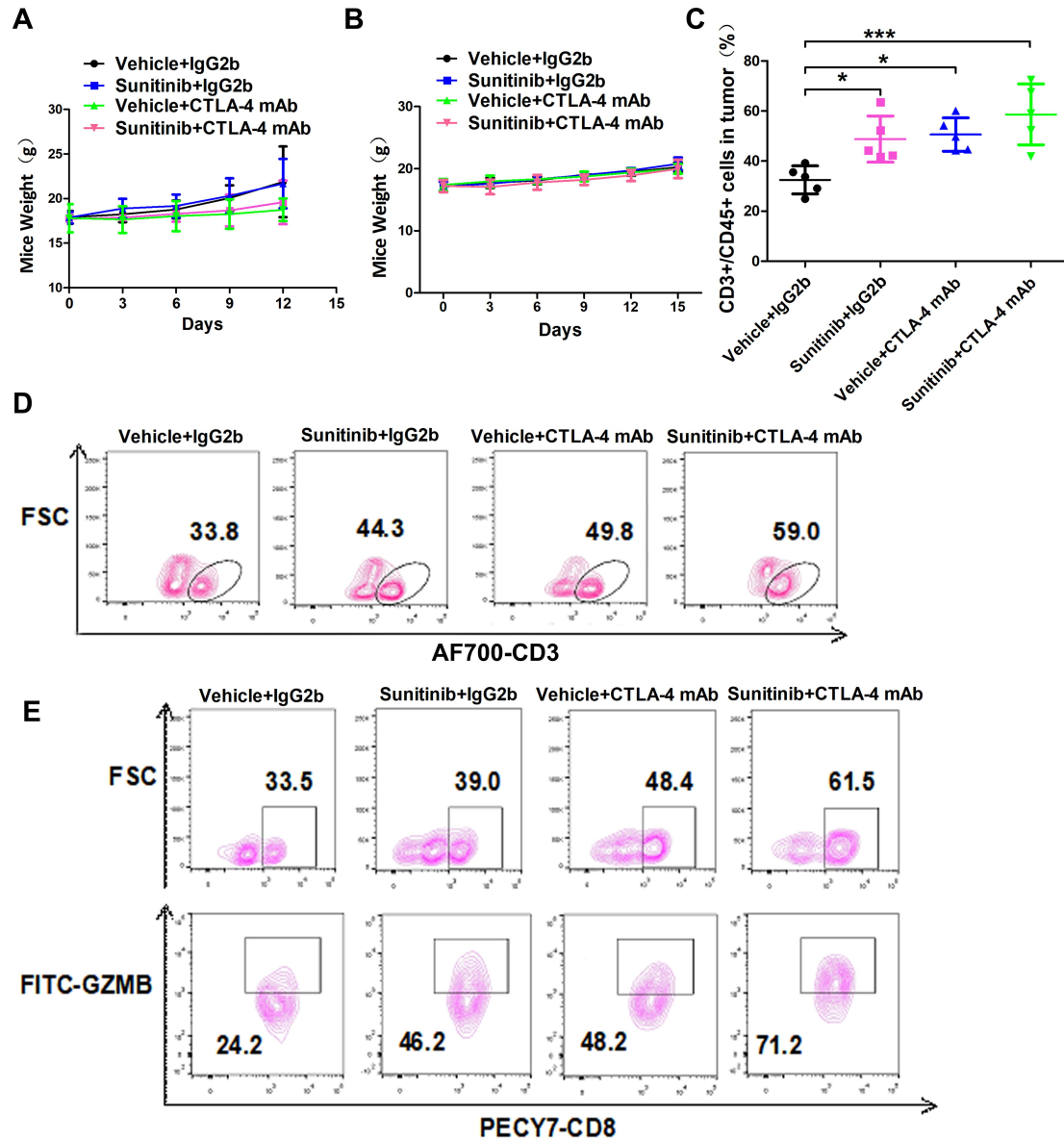


Supplemental Figure 5. PD-L1 decreased by Sunitinib induced p62 in breast and lung cancer cell line.

A. Representative western blot analysis of knockdown p62 in MDA-MB-231 (triple negative breast cancer cell line) and A549 (lung cancer cell line) cells treated with increasing concentrations of Sunitinib (0 to 5 μ M) for 24 hr under IFN- γ exposure.

B. Bar diagram presenting the quantitative analysis of protein expression data from A. The plot was generated from three independent experiments and showed as means \pm SD (**p<0.01, *p<0.05).

Supplemental Figure 6



Supplemental Figure 6. The combination of Sunitinib and anti-CTLA-4 effectively suppresses NSCLC tumor growth *in vivo*

A. The mice body weight of B16F10 tumor model was measured at the indicated time points. n=5 mice per group. Data represent mean±SD, ^{NS}p>0.05.

B. The mice body weight of LLC tumor model was measured at the indicated time points. n=5 mice per group. Data represent mean±SD, ^{NS}p>0.05.

C. The quantification of flow cytometry-based detection of CD45+/CD3+ CTL in the tumor mass from C57/BL6 mice treated with CTLA-4 antibody and/or Sunitinib. n=5 mice per group, data represent mean±SD, *p<0.05, ***p<0.001.

D. Representative profiles of flow cytometry-based detection of CD45⁺ CD3⁺ CD4⁺ CD8⁺ CTL in LLC tumor mass from C57/BL6 mice treated with CTLA-4 antibody and/or Sunitinib.

E. Representative profiles of flow cytometry-based detection of The CD8 (CTL marker) and granzyme B (GZMB) the marker of activity of the T cell in LLC tumor mass from C57/BL6 mice treated with CTLA-4 antibody and/or Sunitinib.